VOL. 3, NO. 6, DECEMBER 2008 ISSN 1819-6608
ARPN Journal of Engineering and Applied Sciences


www.arpnjournals.com

VOLTAGE STABILITY CONSTRAINED ATC COMPUTATIONS IN DEREGULATED POWER SYSTEM USING NOVEL TECHNIQUE

P. Gopi Krishna[1] and T. Gowri Manohar[2]
[1]Department of Electrical and Electronics Engineering, Narayana Engineering College, Nellore, A. P., India
[2]Department of Electrical and Electronics Engineering, S. V. U. College of Engineering, Tirupati, A. P., India
E-Mail: tgmanohar1973@rediffmail.com

ABSTRACT

The voltage stability constrained Available Transfer Capability (ATC) computations are obtained on IEEE 9-bus by running load flow until the voltage collapse point is achieved by enhancing the load in steps with constant power factor. These results are used to train the Neural Network by using Radial Basis Function Neural Network (RBFN) technique. The comparative results of convergence method, L-index method and RBFN network are presented in this study. The results are certainly useful in an online environment of deregulated power system in view of computational simplicity, time and computer memory.

Keywords: voltage stability, ATC, L-index, power flow, RBFN network.

INTRODUCTION

The electrical power system is continuously expanding in size and growing in complexity all over the world with the increase of population and modernization. Therefore the governments have been changing their rules and regulations by allowing the private sectors into the power generation, transmission and distribution (Deregulated Power System). The security in the deregulated power system for the load flow is less, under this insecure environment the power system engineer has to assess the stability constrained ATC in an on-line conditions, apart from the conventional methods so far in use.

The voltage stability studies aim to evaluate the ability of a power system to keep acceptable value of voltages at all nodes either under normal or contingency conditions. Voltage instability involves generation, transmission, and distribution and includes a wide range of phenomena. When a power system is working close to its stability limit, perturbations can easily lead it to a voltage collapse. Different cases of voltage collapse have been observed in power systems and widely analyzed during the past years; they are characterized by a progressive voltage drop in some system buses when load suddenly increases in relatively small quantity in a strongly loaded system. Inadequate reactive power support from generators, reactive sources and transmission lines can lead to voltage instability.

The load-flow analysis of an electrical power system constitutes the basis on which the ATC computations are found. The numerical iterative methods developed in the past and continuously improved by introducing new techniques present a serious drawback when it is required to perform the on line and real time analysis of large size electrical system, related to the convergence needed for the solution. Due to this fact, in recent years interest in the application of soft computing techniques to electrical power systems has rapidly grown. In particular Artificial Neural Networks are good alternative to the classical numerical algorithms. Recently, Radial Basis Function Neural Network (RBFN) has become increasingly popular because of its structural simplicity and training efficiency.

AVAILABLE TRANSFER CAPABILITY

The ATC is a measure of the transfer capability remaining in the physical transmission network for further commercial activity over and above previously committed uses. Mathematically, ATC is defined as the Total Transfer Capability (TTC) [2] less the Transmission Reliability Margin (TRM) [3] and the Capacity Benefit Margin (CBM) [4].

$\therefore$ ATC = TTC – TRM - CBM

TTC is defined as the amount of electric power that can be transferred over the interconnected transmission network in a reliable manner while meeting all of a specific set of defined pre and post-contingency system conditions.

TRM is defined as that amount of transmission transfer capability necessary to ensure that the interconnected transmission network is secure under a reasonable range of uncertainties in system conditions.

CBM is defined as that amount of transmission transfer capability reserved by load serving entities to ensure access to generation from interconnected systems to meet generation reliability requirements.

REPEATED POWER FLOW

The repeated power flow method, which repeatedly solves power flow equations at a succession of points along specified load /generation increment, is used in the work for tracing the fall of voltage. For this method the Newton Raphson method in polar co-ordinates is used.

Newton Raphson Power Flow Solution:
The complex power at bus I is

$$P_i - jQ_i = V_i^* I_i$$

$$Q_i = \sum_{j=1}^{n} |V_i||V_j||Y_{ij}|\sin(\theta_{ij} - \delta_i + \delta_j)$$

$$P_i = \sum_{j=1}^{n} |V_i||V_j||Y_{ij}|\cos(\theta_{ij} - \delta_i + \delta_j)$$

Expanding the last two equations in Taylor's series about the initial estimate and neglecting all higher order terms results in the set of linear equations. In the above equation, bus 1 is assumed to be the slack bus. The Jacobian matrix gives the linearized relationship between small changes in voltage angle $\Delta\delta_i^{(k)}$ and voltage magnitude $\Delta|V_i^{(k)}|$ with a small changes in real and reactive power $\Delta P_i^{(k)}$ and $\Delta Q_i^{(k)}$.

Elements of the Jacobian matrix are the partial derivatives of P_i and Q_i, evaluated at $\Delta\delta_i^{(k)}$ and $\Delta|V_i^{(k)}|$. In short form it can be written as:

$$\begin{bmatrix} \Delta P \\ \Delta Q \end{bmatrix} = \begin{bmatrix} J_1 & J_2 \\ J_3 & J_4 \end{bmatrix} \begin{bmatrix} \Delta\delta \\ \Delta|V| \end{bmatrix}$$

The diagonal elements of J_1, J_2, J_3 and J_4 are found using

$$\frac{\partial P_i}{\partial \delta_i}, \frac{\partial P_i}{\partial |V_i|}, \frac{\partial Q_i}{\partial \delta_i} \;\&\; \frac{\partial Q_i}{\partial |V_i|}$$

Similarly for off-diagonal elements in the place of i, j is used in the denominator terms for the above diagonal elements.

The power residuals, given by:

$\Delta P_i^{(k)} = P_i^{(sch)} - P_i^{(k)}$,

$\Delta Q_i^{(k)} = Q_i^{(sch)} - Q_i^{(k)}$

The new estimates for bus voltages are

$\delta_i^{(k+1)} = \delta_i^{(k)} + \Delta\delta_i^{(k)}$

$|V_i^{(k+1)}| = |V_i^{(k)}| + \Delta|V_i^{(k)}|$

MODELLING OF VOLTAGE INDICATOR (L-Index)

The index of the voltage stability, which is derived from the basic static power flow and Kirchoff's law. A derivation will be given. The index of the voltage stability [3] predicts the voltage problem of the system with sufficient accuracy. This voltage stability index can work well in the static state as well as during dynamic process.

A simple power system is considered, through which the useful index of the voltage stability is derived. As shown in Figure-1, whereby bus 1 is assumed as a generator bus, and bus 2 is a load bus whose voltage behavior will be our interest.

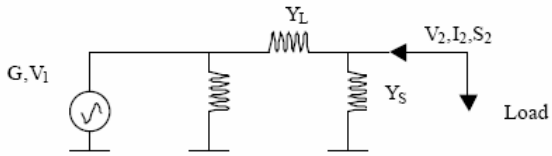

Figure. 1. Single generator and Load system

This simple system can be described by the following equations (where the dot above a letter represents a vector)

$$\dot{I}_2 = \dot{V}_2 \dot{Y}_S + (\dot{V}_2 - \dot{V}_1)\dot{Y}_L = \frac{\overset{*}{S}_2}{\overset{*}{V}_2} \quad (1)$$

$$\overset{*}{S}_2 = V_2^{\,2}\dot{Y}_S + V_2^{\,2}\dot{Y}_L - \overset{*}{V}_2\dot{V}_1\dot{Y}_L$$

$$= V_2^{\,2}\dot{Y}_{22} + \dot{V}_0\overset{*}{V}_2\dot{Y}_{22} \quad (2)$$

$$Here\ \dot{Y}_{22} = \dot{Y}_S + \dot{Y}_L$$

$$and\ \dot{V}_0 = -\frac{\dot{Y}_L}{\dot{Y}_L + \dot{Y}_S}\dot{V}_1 \quad (3)$$

All the buses can be divided into two categories Generator bus (PV bus and Slack bus) and Load bus (PQ bus). Because the voltage stability problem is reactive power relative problem, and the generator bus can provide the reactive power to support the voltage magnitude of the bus.

The power system can be expressed in the form through Kirchoff's Law:

$$I_{System} = \begin{bmatrix} I_L \\ I_G \end{bmatrix} = \begin{bmatrix} Y_{LL} & Y_{LG} \\ Y_{GL} & Y_{GG} \end{bmatrix} \begin{bmatrix} V_L \\ V_G \end{bmatrix} = Y_{System} V_{System} \longrightarrow (4)$$

Subscript L means Load bus, and G means Generator bus.

$$\begin{bmatrix} V_L \\ I_G \end{bmatrix} = \begin{bmatrix} Z_{LL} & -Z_{LL}Y_{LG} \\ Y_{GL}Z_{LL} & Y_{GG} - Y_{GL}Z_{LL}Y_{LG} \end{bmatrix} \begin{bmatrix} I_L \\ V_G \end{bmatrix} \longrightarrow (5$$

Here, $Z_{LL} = Y_{LL}^{-1}$

For any load bus j□*L* through the equation (5), the voltage of the bus is known as

$$\dot{V}_j = \sum_{i \in L} Z_{ji}\dot{I}_i + \sum_{k \in G} A_{jk}\dot{V}_k \longrightarrow (6)$$

$$A = -Z_{LL}Y_{LG}$$

This can be expressed as the form

$$V_j^{\,2} + \dot{V}_{0j}\overset{*}{V}_j = \frac{\overset{*}{S}_j'}{Y_{jj}'} \longrightarrow (7)$$

Substituting equivalent V_{0j} , $S_j^{'}$ and $Y_{jj}^{'}$, we have

$$\dot{V}_{0j} = -\sum_{k \in G} A_{kj} V_k \quad \rightarrow (8)$$

$$Y_{jj}' = \frac{1}{Z_{jj}} \quad \rightarrow (9)$$

$$\dot{S}_j' = (\sum_{i \in L} \frac{\overset{*}{Z}_{ji} \dot{S}_i}{\overset{*}{Z}_{jj} \overset{*}{V}_i}) * \dot{V}_j = \dot{S}_j + (\sum_{\substack{i \in L \\ i \neq j}} \frac{\overset{*}{Z}_{ji} \dot{S}_i}{\overset{*}{Z}_{jj} \overset{*}{V}_i}) * \dot{V}_j \quad (10)$$

Hence, we see that the voltage of the load bus j is affected by an equivalent complex power and by an equivalent generator part V_{0j}. To compare the equation (7) and (2), we can observe that they have an identical form, and the voltage stability of the multi-bus system has been equivalent to a simple single generator and load system. The indicator of the voltage stability of the load bus j will be easily obtained.

$$Indicator_j = \left| 1 + \frac{\dot{V}_{0j}}{\dot{V}_j} \right| = \left| \frac{\overset{*}{S}_j'}{V_j^2 \overset{*}{Y}_{jj}'} \right| = \frac{S_j'}{V_j^2 Y_{jj}}$$

For the system

$$Indicator_{system} = \underset{j \in L}{Max}(Indicator_j)$$

Thereby it is clear that the indicator of the voltage stability at a load bus mainly influenced by the equivalent load, which has two parts: the load at bus j itself, and the 'contributions' of the other load buses (shown in equation 10). When the load at a load bus changes, it will influence the indicator [8]. On the other words, the voltage stability problem is a system-wide problem, not a local problem.

RADIAL BASIS FUNCTION NEURAL NETWORK

RBFN [5] network consists of 3-layers: input layer, hidden layer, and output layer, as shown in Figure-2. The neurons in hidden layer are of local response to its input and known as RBF neurons, while the neurons of the output layer only sum their inputs and are called linear neurons. Radial basis function network (RBFN), which has nonlinear mapping capability, has become increasingly popular in recent years due to its structural simplicity and training efficiency. A potential advantage of RBFN is its ability to augment new training data without the need for retraining.

The RBFN finds the design of neural network as a curve-fitting (approximation) problem in a high-dimensional space that provides the best fit to the training data. The hidden units provide a set of functions that constitute an arbitrary basis for the input patterns when they are expanded into the hidden-unit space. These functions are called radial basis functions.

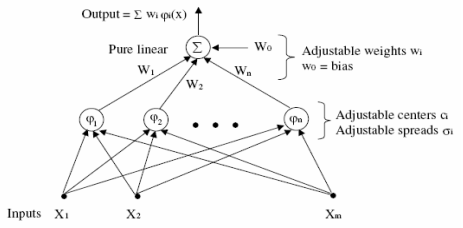

Figure-2. Architecture of radial basis function network.

TEST SYSTEM AND RESULTS

The voltage stability constrained ATC computations in the deregulated power system are achieved through three methods on following test system shown in Figure-3. The three methods are:
(1) Convergence method (2) L-Index method [6] and (3) RBFN Network.

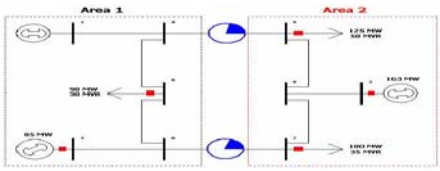

Figure-3. 9-bus system simulation test case.

The IEEE 9-bus data [7] is considered for the above test system and it has been divided into two areas to consider the deregulated environment, in that bus-1 is the slack bus, all other generator's active power are kept constant except for the slack bus generator. So that the power increased in the load would be drawn from the slack bus. The flow limits in all transmission lines are assumed to be infinity.

Case scenarios for 1st method (Convergence)

In this method, the voltage stability constrained ATC [9] is obtained using repeated power flow method that uses the Newton's Raphson method in polar co-ordinates to run the power flow on the proposed IEEE 9-bus system as shown in Figure-3, and whose summary is described as, the normal base loading at load buses are:

Bus 5: 90 + j 30 MVA; Bus 7: 100 + j 35 MVA
Bus 9: 125 + j 50 MVA

Buses 1 to 3 are generation buses; there are no generators or loads at buses 4, 6 and 8.
Four case scenarios have been simulated in the first method.

Case-1. Increasing the load at bus 7

The first test is done by increasing the load at bus 7 to increase the power transfer from area 1 to area 2. The load at bus 7 is increased gradually with equal increments and with constant power factor, until the Newton's Raphson method is not converged. After this point decrease the load at bus 7 with small steps that is less than the previous increased steps until the NR method is

converged. The results of the simulation are shown in Table-1.

Table-1. Increasing the load at bus-7.

#	Load at bus 7 (S_7) in MVA	Voltage at bus 7 (V_7) in p.u	Converged
1.	100+J35	0.987∠0.378	YES
2.	200+j70	0.945∠-13.31	YES
3.	300+j105	0.884∠-29.155	YES
4.	400+j140	0.776∠-51.732	YES
5.	450+j157.5	0.421∠30.964	NO
6.	**442+j154.7**	**0.627∠-76.988**	**YES**
7.	442.5+j154.87	0.626∠-77.231	NO

TTC = 442 + 125 = 567MW
ATC = 567 – 225 = 342 MW
Base case loads at Bus 5: 90 + j 30 MVA
At Bus 7: 100 + j 35 MVA
At Bus 9: 125 + j 50 MVA

Case-2. Increasing the load at bus 9

Similar to the case-1, the load is varied at bus-9; the results of the simulation are shown in Table-2.

Table-2. Increasing the load at bus-9.

#	Load at bus 9 (S_9) in MVA	Voltage at bus 9 (V9) in p.u	Conver-ged
1.	125+J50	0.958∠-4.458	YES
3.	225+j90	0.894∠-13.123	YES
4.	325+j130	0.788∠-24.705	YES
5.	**379.5+j151.8**	**0.619∠-39.513**	**YES**
6.	380+j152	0.596∠-41.303	NO

TTC = 379.5 + 100 = 479.5 MW
ATC = 479.5 - 225 = 254.5 MW

Case-3. Increasing the load at bus 7 with contingency

The third test is done by running the power flow with a contingency. The branch line between bus 6 and 7 is shutoff, which means the power flow from area 1 and 2 is only through the line branch between bus 4 and 9. The results of the simulation are shown in Table-3.

Table-3. Increasing the load at bus-7 with contingency.

#	Load at bus 7 (S_7) in MVA	Voltage at bus 7 (V_7) in p.u	Converged
1.	100 + j 35	0.948∠-4.186	Yes
2.	200 + j 70	0.833∠-30.678	Yes
3.	250 + j 87.5	0.690∠-53.201	Yes
4.	**256.5 + j 89.775**	**0.626 ∠-60.797**	**Yes**
5.	257 + j 89.95	0.602 ∠-63.184	N0

TTC = 256.5 + 125 = 381.5 MW
Base Case = 225.0
ATC = 381.5 – 225 = 156.5 MW

Case-4. Increasing the load at bus 9 with contingency

Similarly as in case-3 the load is increased at bus 9 instead of bus 7. The results of the simulation are shown in Table-4.

Table-4. Increasing the load at bus-9 with contingency.

#	Load at bus 9 (S_9) in MVA	Voltage at bus 9 (V_9) in p.u	Converged
1	125+j50	0.952∠-5.731	YES
2	250+j100	0.859∠-18.375	YES
3	350+j140	0.645∠-40.164	YES
4	355+j142	0.607∠-43.614	NO
5	**350.5+j140**	**0.635∠-41.083**	**YES**

TTC = 350.5 + 100 = 450.5 MW
ATC = 450.5 – 225 = 225.5 MW

Case scenarios for 2nd method (Index)

In the second method, the approximate voltage collapse point is fastly identified with index of bus 5, 7 and 9 and hence approximate value (near to actual value) of voltage stability constrained ATC is obtained on the same IEEE 9-bus system. Four case scenarios have been simulated for the second method.

Case-1. Index of bus 5, 7 and 9 for variation of load at bus 7 without contingency

As seen in Figure-4, index L approaches one at the collapse point. For this simulation, the load at bus 7 is varied from 100 + j 35 MVA and load at bus 9 is taken as 125 + j50 MVA and the load at bus 5 is taken as 90 + j30 MVA. As seen in the following figure the voltage stability constrained load flow is **435.92MW** at the precise voltage collapse point. Therefore,
TTC = 435.92 + 125 = 560.92 MW
ATC = TTC – Base case load
ATC = 560.92 – 225 = 335.92 MW

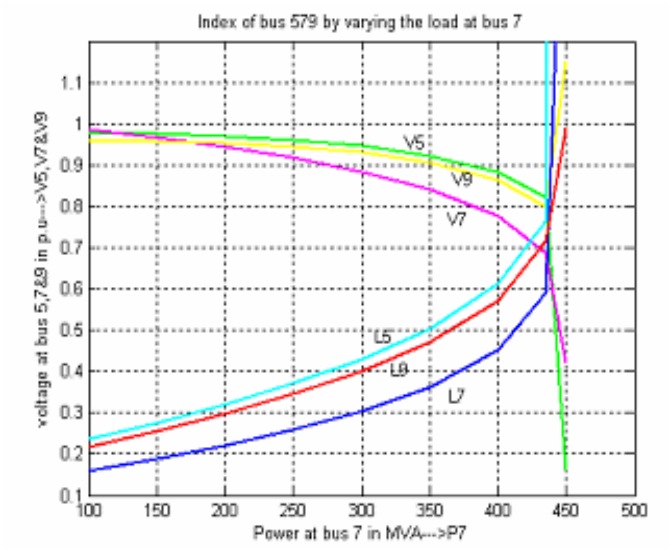

Figure-4. Index of buses 5, 7&9 by varying the load at bus 7 with out contingency.

Case-2. Index of bus 5, 7 and 9 for variation of load at bus 9 without contingency

Similarly as in case 1 of (B) load is increased at bus 9. As seen in the Figure-5 the voltage stability constrained load flow is **365.8 MW** at the first voltage collapse. Therefore,

TTC = 365.8 + 100 = 465.8 MW

ATC = TTC – Base case load

ATC = 465.8 – 225 = 240.8 MW

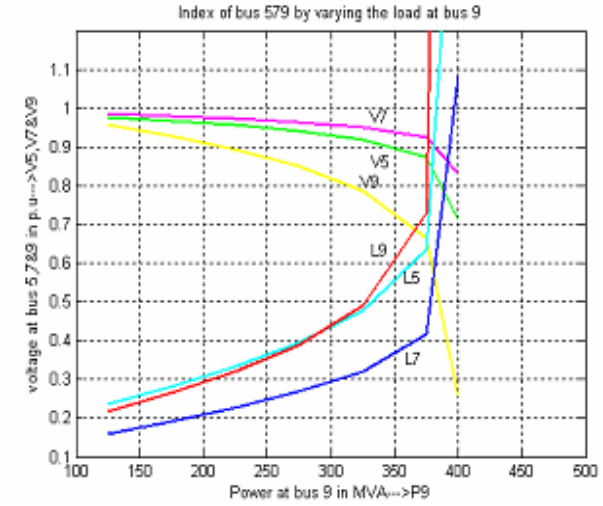

Figure-5. Index of buses 5, 7&9 by varying the Load at bus-9 with out contingency.

Case-3. Index of bus 5, 7 and 9 for variation of load at bus 7 with contingency

The branch line between bus 6 and 7 is shut off, which means the power transferred from area 1 and 2 is only through the line branch between bus 4 and 9. As seen in the Fig.6 the voltage stability constrained load flow is 252.5 MW at first voltage collapse. Therefore,

TTC = 252.5 + 125 = 377.5 MW

ATC = TTC – Base case load

ATC = 377.5 – 225 = 152.5 MW

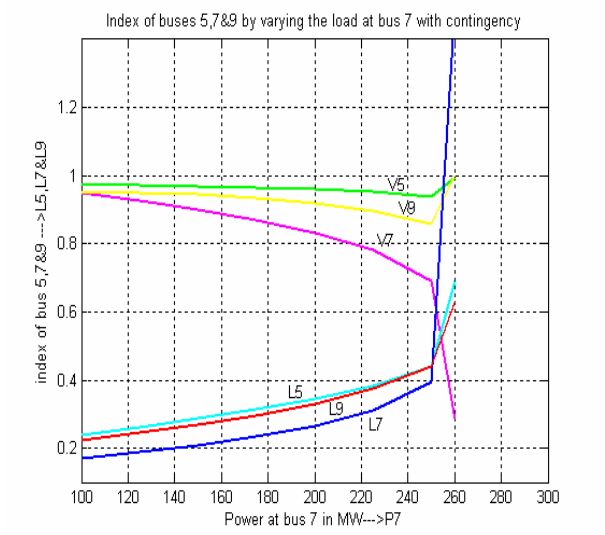

Figure-6. Index of buses 5, 7 and 9 by varying the load at bus-7 with contingency.

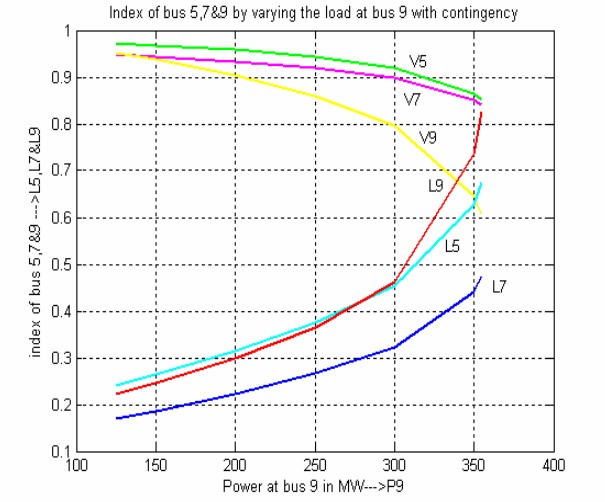

Figure-7. Index of buses 5, 7 and 9 by varying the load at bus 9 with contingency.

Case-4. Index of bus 5, 7 and 9 for variation of load at bus 9 with contingency

Similarly as in case 3 of (B) load is increased at bus 9.As seen in the Figure-7 the voltage stability constrained load flow is 339.37 MW at first voltage collapse. Therefore,

TTC = 339.37 + 100 = 439.37 MW

ATC = TTC – Base case load

ATC = 439.37 – 225 = 214.37 MW

Case scenarios for 3rd method (RBFN Network)

In this method, the input-output patterns for training the proposed RBFN network are generated from the repeated power flow algorithm. The input to the

proposed RBFN network is the real power demand of the system. The outputs are the voltage magnitudes, angles at different buses and convergence status. The trained RBFN network is shown in Figure-8.

The simulation results of voltage stability constrained ATC using RBFN is shown in Table-5 along with the results of all cases of above two methods.

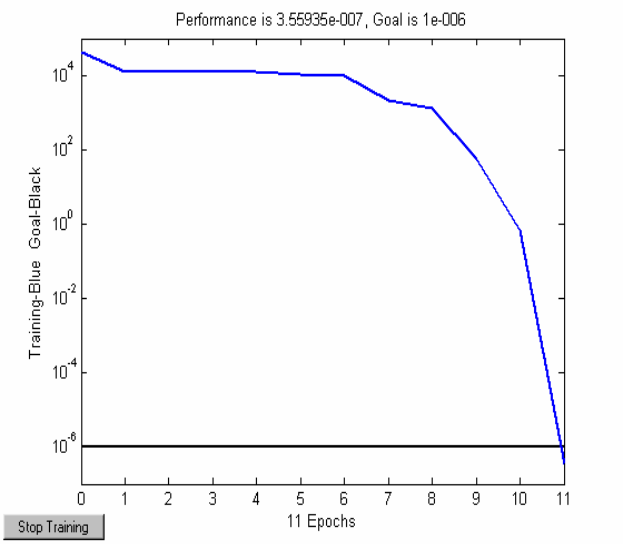

Figure-8. Trained curve fitting RBFN network with the performance goal of $1e^{-6}$.

Table-5. Comparison of voltage stability constrained load flow using 3 methods.

Method	Case	Stability constrained ATC in MW
1st (Convergence)	Case 1	342.0
	Case 2	254.5
	Case 3	156.5
	Case 4	225.5
2nd (L-Index)	Case 1	335.92
	Case 2	240.8
	Case 3	152.5
	Case 4	214.37
3rd (RBFN Network)	Case 1	341.5
	Case 2	253.5
	Case 3	155.0
	Case 4	224.5

CONCLUSIONS

In this paper, the voltage stability constrained ATC computations on IEEE 9-bus are achieved for the different case scenarios with and without contingencies using convergence method, L-index and RBFN network. In the case of convergence method, to obtain the results, the requirement of time is more and the process is tedious, but the results are accurate. In the L-index method, the obtained results are approximate to actual values, but which are acceptable in the emergency conditions due to the requirement of time is less and the process is not tedious in obtaining the results. The results obtained through the RBFN network will not involve any mathematical equations which are used in the first two methods, even then the accuracy in results is almost equal with convergence method and observed that this accuracy is depends on how well the conventional input data available near to the presented problem to train RBFN network effectively and the computer memory, computational CPU time are less and process obtaining the results is simple. Therefore under contingencies the RBFN network is best suitable for online monitoring/evaluating the voltage stability constrained ATC in the deregulated power system.

REFERENCES

[1] Garng M. Huang, Liang Zhao. Measurement based Voltage Stability Monitoring of Power system. Dept. of Electrical Engineering, Texas A & M University.

[2] Garng M. Huang, Ali Abur. Voltage Security Margin Assessment. Texas A & M University, Power Systems Engineering Research Center.

[3] Margins Yan Ou. and Chanan Singh. 2002. Assessment of Available Transfer Capability. IEEE Transactions on Power Systems. Vol. 17, No. 2.

[4] Ashwani Kumar, S.C. Srivastava and S.N. Singh. Available transfer capability assessment in a competitive electricity market using a bifurcation approach. IEE Proceedings online No. 20040076, DOI: 10.1049/ip-gtd: 20040076.

[5] Peter W. Sauer. 1997. Technical Challenges of Computing Available Transfer Capability. In: Electric Power Systems, Proceedings of 30th Annual Hawaii International Conference on System Sciences.

[6] Peter W. Sauer. 1998. Alternatives for calculating Transmission Reliability Margin in Available Transfer Capability. IEEE Transactions. January.

[7] G.C. Ejebe *et al.* 1998. Available Transfer Capability Calculations. IEEE Transactions on Power Systems. Vol. 13, No. 4, November.

[8] Gabriel C. Ejebe *et al.* 2002. Fast Calculation of Linear Available Transfer Capability. IEEE Transactions on Power Systems. Vol. 15, No. 3, August.